Ergonomics

ISSN: (Print) (Online) Journal homepage: https://www.tandfonline.com/loi/terg20

A design tool to estimate maximum acceptable manual arm forces for above-shoulder work

David Rempel & Jim Potvin

To cite this article: David Rempel & Jim Potvin (2022) A design tool to estimate maximum acceptable manual arm forces for above-shoulder work, Ergonomics, 65:10, 1338-1351, DOI: 10.1080/00140139.2022.2030806

To link to this article: https://doi.org/10.1080/00140139.2022.2030806

© 2022 The Author(s). Published by Informa UK Limited, trading as Taylor & Francis Group.

Published online: 28 Feb 2022.

Submit your article to this journal

Article views: 1447

View related articles

View Crossmark data

Full Terms & Conditions of access and use can be found at https://www.tandfonline.com/action/journalInformation?journalCode=terg20

ERGONOMICS
2022, VOL. 65, NO. 10, 1338–1351
https://doi.org/10.1080/00140139.2022.2030806

Taylor & Francis
Taylor & Francis Group

ARTICLE

OPEN ACCESS Check for updates

A design tool to estimate maximum acceptable manual arm forces for above-shoulder work

David Rempel[a] and Jim Potvin[b]

[a]Department of Bioengineering, University of California, Berkeley, CA, USA; [b]McMaster University, Hamilton, ON, Canada

ABSTRACT

There is a need for design criteria for above-shoulder work to prevent shoulder fatigue and supraspinatus injuries. A tool is developed to estimate maximum acceptable manual arm forces for above-shoulder work based on 25th % female strength with adjustments for supraspinatus tendon impingement and shoulder fatigue. The tool equations are presented along with tables of maximum acceptable manual arm forces in 77 locations in the 3 D space above the shoulder that accommodates a 50th % female reach. The largest acceptable anterior force, 140.3 N, occurs at shoulder height, 0.5 m anterior to the shoulder. The largest acceptable superior force, 84.4 N, occurs at shoulder height, 0.1 m anterior and 0.2 m medial to the shoulder. The new tool provides design criteria for arm exertions at a higher level of detail than prior ergonomic tools, making it useful for engineers. Based on sensitivity analyses, the tool is robust to parameter assumptions.

Practitioner summary: Above-shoulder work is associated with increased risk for shoulder fatigue and injuries. A new tool is developed that estimates maximum acceptable manual arm forces for work at or above shoulder height. The tool can be used to design acceptable above-shoulder work so that it can be accomplished by most workers.

Abbreviations: AFF: arm force field; AP: anterior/posterior; DC: duty cycle; GH: glenohumeral angle; HT: humerothoracic angle; LM: lateral/medial; MAE: maximum acceptable effort; MAF: maximum acceptable force; MAS: manual arm strength; MVC: maximum voluntary contraction; N: newton; OCRA: occupational repetitive action; R: reach distance; RMS: root means square; RULA: rapid upper limb assessment; SF: scale factor; SI: superior/inferior; ST: scapulothoracic angle; T: thoracic

ARTICLE HISTORY
Received 30 June 2021
Accepted 19 November 2021

KEYWORDS
Overhead work; rotator cuff; musculoskeletal disorders; work design; supraspinatus tears

KEY POINTS

- A new design tool is introduced that estimates maximum acceptable hand forces for specific locations above the shoulder.
- This above-shoulder tool is based on a 50th percentile female anthropometry and 25th percentile female manual arm strength.
- These base strengths are multiplied by scaling factors that adjust for subacromial impingement and fatigue.
- The tool was shown to be robust based on sensitivity analysis.

1. Introduction

Shoulder pain is a common and increasing problem among workers, affecting 18–26% during their working life (Linaker and Walker-Bone 2015). Shoulder fatigue, pain and injuries can limit the ability to perform hand intensive work and can lead to high levels of disability, health care costs, and lost worktime and reduced work quality (Jakobsen et al. 2018; Sirén et al. 2019). Common occupational shoulder injuries include supraspinatus tendon tears, subacromial impingement, biceps tendonitis, and shoulder bursitis.

Recent systematic reviews have found that shoulder disorders are associated with the workplace risk factors of working with the hand above the shoulder, forceful hand exertion, and shoulder load (van der Molen et al. 2017; Rijn et al. 2010). The reviews included studies of specific disorders, confirmed with imaging or during surgery, such as supraspinatus tendonitis and subacromial impingement, and also studies of shoulder disorders with a diagnosis based on a physical examination. A recent study of workers who received surgery for subacromial impingement

CONTACT David Rempel david.rempel@ucsf.edu Department of Bioengineering, University of California, Berkeley, 1301 S. 46th Street, UC RFS Building 163, Richmond, CA 94804, USA

© 2022 The Author(s). Published by Informa UK Limited, trading as Taylor & Francis Group.
This is an Open Access article distributed under the terms of the Creative Commons Attribution-NonCommercial-NoDerivatives License (http://creativecommons.org/licenses/by-nc-nd/4.0/), which permits non-commercial re-use, distribution, and reproduction in any medium, provided the original work is properly cited, and is not altered, transformed, or built upon in any way.

identified arm elevation, forceful shoulder exertion, and rapid shoulder movements as risk factors (Dalbøge et al. 2018). Shoulder muscle fatigue, shoulder pain, and overuse injuries are commonly associated with overhead assembly work in manufacturing, such as aircraft and auto assembly (Punnett et al. 2000). Shoulder muscle loading is highly dependent on hand location and force direction during submaximal efforts performed above the shoulder (Chopp, Fischer, and Dickerson 2010). Increasing age also contributes to risk (Hallman et al. 2018).

Occupational supraspinatus tears are a common and disabling shoulder injury which are associated with degenerative changes to the tendon, likely due to repeated, forceful impingement (e.g. compression and shear) of the tendon between the coracoacromial arch and the head of the humerus (Pandey and Willems 2015). At approximately 60° of humeral flexion or abduction, relative to the scapula (glenohumeral rotation), the supraspinatus tendon will begin to be compressed beneath the coracoacromial arch (Luo et al. 1998; Yamamoto et al. 2010). Elevations above this angle will lead to progressively higher compression and shear forces on the tendon. Furthermore, during above shoulder hand activities, the degree of compression, shear and tension increases with increasing hand force (Miller et al. 2019; Zheng et al. 2017; Dickerson, McDonald, and Chopp-Hurley 2020).

Supraspinatus tendon compression, shear, and tension can also increase when the deltoid muscle, which is the primary muscle for abducting and flexing the shoulder, becomes fatigued. The supraspinatus muscle stabilises the shoulder and assists in abduction when the deltoid is fatigued. For above-shoulder work, once the deltoid fatigues, and the force it can generate is reduced, workers will shift to a shrug posture to reduce loads on the shoulder muscles (Fuller et al. 2009). With deltoid muscle fatigue, the humerus is translated in the superior direction and this increases supraspinatus compression (Dickerson, McDonald, and Chopp-Hurley 2020). Shoulder fatigue may also lead to less scapular rotation during upper arm rotation, and this may further increase impingement (McQuade, Dawson, and Smidt 1998, McQuade, Wei, and Smidt 1995). Muscle fatigue is related to the level of muscle load relative to strength (e.g. Maximum Voluntary Contraction, MVC%) and the duration of muscle load (e.g. duty cycle). Fatigue can be controlled by following recommendations from the Maximum Acceptable Effort (MAE) equation (Potvin 2012) or the ACGIH Upper Limb Localized Fatigue Threshold Limit Value (ACGIH 2016). Repetitive, hand intensive work should be designed so that these guidelines are not exceeded.

Shoulder biomechanical models provide insight into understanding how supraspinatus tendon compression and torsional forces are related to hand and shoulder postures, hand loads, and muscle forces. As the humerus is flexed or abducted, the scapula (and the attached acromion) also rotates, but to a lesser degree. Specifically, when the upper arm is rotated (flexed or abducted) relative to the torso (humerothoracic rotation) approximately 2/3 of the rotation is due to the humerus moving relative to the scapula (glenohumeral rotation) and 1/3 is due to the scapula moving relative to the torso (scapular rotation) (Lee et al. 2020). This 2:1 ratio, between glenohumeral and scapulothoracic rotation, is called 'scapulohumeral rhythm' or 'shoulder rhythm' and can be used to estimate the glenohumeral angle from the humerothoracic angle. In the workplace, ergonomists can readily measure the humerothoracic angle, the angle of the upper arm relative to the torso, but knowledge of the underlying glenohumeral angle is necessary to estimate the degree of impingement.

There are no existing ergonomics assessment tools for designing above-shoulder work that incorporate worker strength capacity, fatigue, and impingement. RULA generates a risk score for musculoskeletal disorders that assigns risk points to four levels of shoulder posture (<20°, 20°–45°, 45°–90°, >90°) and 3 levels of hand loads (<2 kg, 2–10 kg, and >10 kg) (McAtamney and Corlett 1993). External rotation of the shoulder adds an additional risk point. The ISO standard for manual handling (ISO 2007) incorporates the OCRA risk assessment method (Occhipinti 1998) and identifies a risk for shoulder disorders if (1) the upper arm is rotated to >80° for >10% of cycle time or >2 actions/min, or (2) the arm is rotated from 45° to 80° for >33% of cycle time or >10 actions/min. Both RULA and OCRA are relatively crude risk assessment tools that do not provide a hand force limit related to hand position, and, therefore, are not readily usable for the design of over shoulder work. Ergonomic software packages (e.g. 3DSSPP (Regents of the University Michigan, Ann Arbour, MI), Process Simulate (Siemens, Ann Arbour, MI) and Santos (SantosHuman Inc., Coralville, IA)) allow mannequins of workers to be manipulated to almost any arm posture to estimate arm strength, but these tools do not consider impingement or fatigue. In addition, the predicted strengths of these packages have some limitations (Hall et al. 2021). A new shoulder tool estimates cumulative shoulder tendon damage by using 3DSSPP strength prediction and shoulder moment based on hand posture and adds repetitions per workday as a fatigue failure

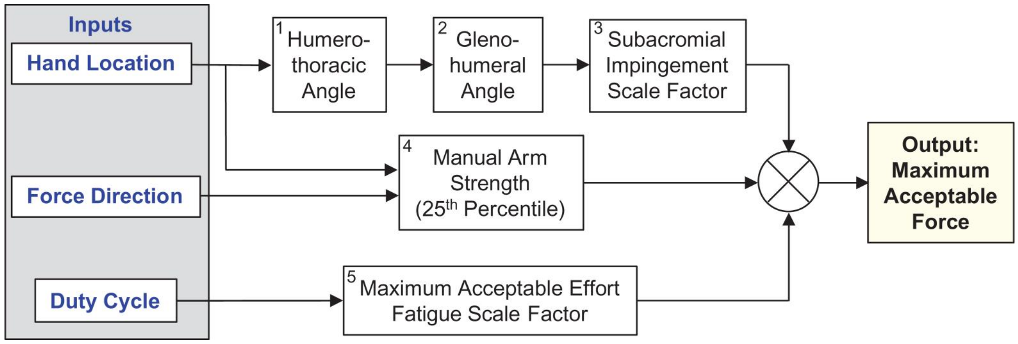

Figure 1. Flowchart of the five models incorporated into the above-shoulder tool. The inputs are hand location relative the shoulder, hand force direction, and duty cycle. In the current application, the hand location is combined with 50th percentile female arm segment lengths to estimate humerothoracic angle, glenohumeral angle and the subacromial impingement scale factor. The force direction and hand location are used to estimate the 25th percentile female manual arm strength. The duty cycle is used to estimate a scale factor for maximum acceptable effort to control for fatigue. The 25th percentile manual arm strength is multiplied by the subacromial impingement scale factor and the fatigue scale factor to calculate the maximum acceptable force for above-shoulder work.

element (Hani et al. 2021). The tool does not incorporate impingement, uses only one strength regardless of hand location, and does not consider muscle fatigue.

The objective of this paper is to develop a new tool to guide the design of above-shoulder work based on the strength capability of workers with adjustments to prevent supraspinatus tendon impingement and shoulder muscle fatigue. The tool uses inputs of hand location relative to the shoulder to estimate maximum acceptable forces that can be applied by the hand that will protect most workers. The forces are scaled down with increasing shoulder rotation angles that are associated with increasing subacromial impingement, to reduce compression and shear of the supraspinatus tendon. The forces are also scaled down to prevent muscle fatigue associated with repetitive tasks. Safety personnel can use the tool to identify work tasks that should be considered for redesign. Engineers can use the tool to proactively design new above-shoulder tasks. The ultimate purpose of the tool is to prevent shoulder fatigue, shoulder pain, and shoulder injuries, such as supraspinatus tears.

2. Methods

2.1. Tool structure and development

The tool consists of several components that include geometric, biomechanical, and empirical models of the shoulder and muscle complex. The tool estimates maximum arm force based on, (1) a linked-segment model that estimates humerothoracic angle based on hand location and assumptions about segment lengths and elbow orientation; (2) a model of the scapulohumeral rhythm to estimate glenohumeral rotation based on humerothoracic angle; (3) a model to determine a scale factor to limit subacromial impingement based on glenohumeral angle; (4) a model of the anterior, posterior, superior, inferior, medial and lateral manual arm strengths based on hand location relative to the shoulder; and (5) a model to determine a scale factor to control muscle fatigue based on the task duty cycle (Figure 1). For ease of use, the outputs are presented in look-up tables.

2.1.1. Hand locations matrix

We evaluated a matrix of hand locations at or above shoulder height with coordinates relative to the shoulder joint location. We assumed a 50th percentile female body mass of 73.5 kg and stature of 1.619 m based on NHANES 2015–2018 (Fryar et al. 2021) for the age range from 20 to 69 years. The upper arm (shoulder to elbow), forearm (elbow to wrist) and hand (wrist to the 3rd digit MCP joint, referred to in this paper as the 'knuckle') segment lengths were assumed to be 18.2%, 14.4% and 4.4% of stature (3DSSPP v7.1.0, University of Michigan, Ann Arbour, MI) and produced respective lengths of 0.294, 0.233 and 0.072 m, and a total reach of 0.599 m. The hand segment was always assumed to be parallel to the forearm segment (e.g. wrist in the neutral posture). Hand locations were defined by the knuckle coordinate. We assumed an upright trunk and hand locations were assessed in a 3 D matrix with every combination of lateral/medial (LM) location from −0.2 m medial to 0.4 m lateral to the shoulder (step = 0.2 m, $n = 4$), anterior/posterior (AP) location from 0.1 to 0.5 m anterior to the shoulder (step = 0.1 m, $n = 5$), and superior/inferior (SI) location from 0.0 to 0.5 m superior to the shoulder (steps = 0.1 m, $n = 6$) for a total of 120 hand locations in the full matrix (Figure 2).

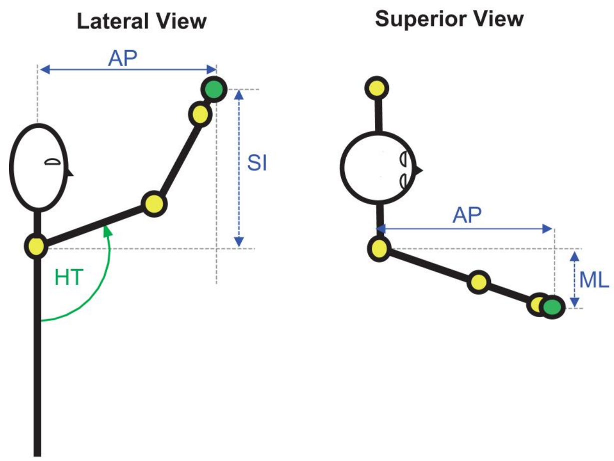

Figure 2. Illustration of the superior/inferior (SI), anterior/posterior (AP) and medial/lateral (ML) coordinates of the knuckle and the calculation of humerothoracic angle (HT). The wrist was always assumed to be n the neutral posture.

The reach distance (R) was calculated as the distance between the shoulder and knuckle. The studies described by La Delfa and Potvin (2017), and used later in Section 2.1.5 to estimate manual arm strength, used reaches that ranged from 0.236 to 0.533 m, so we limited the reaches to be between 0.20 and 0.55 m. Of the 120 locations in the full 3D matrix, 77 were within that reach range so only that subset of hand locations was included in subsequent analyses.

2.1.2. Humerothoracic angles

For each of the 77 hand locations identified, a plane was created with the upper arm segment, the forearm/hand segment, and the reach vector (shoulder to knuckle), and this plane was assumed to be oriented vertically. Using the Cosine Law, the resultant angle between the upper arm segment and upright trunk was calculated to represent the humerothoracic (HT) angle for each hand location. The HT angle was measured between the flexion and abduction planes and was calculated to be the angle between the reach vector with the vertical trunk segment (horizontal is 90°) minus the angle between the reach vector and the upper arm segment. As noted, the reach distance (R) was calculated as the resultant distance from the shoulder to knuckle. The HT angle was calculated with Equation (1), using the upper arm length (0.294 m), forearm/hand length (0.305 m), variable reach distance (R) and the variable coordinates of the knuckle with respect to the shoulder, using the lateral/medial (LM), anterior/posterior (AP) and superior/inferior (SI) location of the knuckle.

$$\mathrm{HT} = 90 + \arctan\left[\frac{\mathrm{SI}}{\sqrt{\mathrm{LM}^2 + \mathrm{AP}^2}}\right] - \arccos\left[\frac{0.305^2 - \mathrm{R}^2 - 0.294^2}{-2(\mathrm{R})(0.294)}\right] \quad (1)$$

2.1.3. Scapulohumeral rhythm

Scapulohumeral rhythm has been measured using many methods, including 2D tracking of bone landmarks with X-rays (e.g. Poppen and Walker 1976), in 3D with external tracking over the skin with electromagnetic devices (e.g. McClure et al. 2001), with probes (e.g. de Groot and de Brand, 2001) and with optical motion capture markers (e.g. Grewal and Dickerson 2013). However, only the four *in vivo* studies that directly tracked 3D scapular and humeral bone motions were considered for estimating the scapulohumeral rhythm in the scapular plane (Kon et al. 2008; Lee et al. 2020; Ludewig et al. 2009; Matsuki et al. 2011). Across the four studies, the average glenohumeral (GH) rotation (degrees) was calculated at each humerothoracic (HT) angle from 10° to 140° in increments of 10° (Figure 4).

Both a linear and a 2nd order polynomial regression equation were fit to model glenohumeral rotation as a function of humerothoracic rotation. The second order polynomial regression Equation (2) was used in the model since it provided a slightly better fit ($p < 0.0001$, $r^2 = 0.999$, RMS difference $= 0.17°$) than the linear equation ($p < 0.0001$, $r^2 = 0.999$, RMS difference $= 0.67°$).

$$\mathrm{GH} = 0.655(\mathrm{HT}) + 0.0002717(\mathrm{HT}^2) \quad (2)$$

2.1.4. Subacromial impingement scale factor

As the upper arm is elevated in abduction or flexion the humerus rotates and moves upward and, at some point in elevation, the humeral head comes in contact with the coracoacromial arch and begins to compress or impinge on the supraspinatus tendon. With increasing humerothoracic rotation, there is an increase in glenohumeral rotation, which further decreases the subacromial space and increases tendon compression and shear (Figure 3). The contact pressure on the supraspinatus tendon has been measured directly during surgery with pressure transducers while the shoulder was passively abducted (Hyvönen, Lantto, and Jalovaara 2003). The pressure has also been measured in cadavers, where the scapula was fixed and the humerus was rotated in abduction and flexion (GH rotation) while contact pressure was measured (Gupta and Lee 2005; Hughes, Green, and Taylor 2012; Muraki et al. 2017; Payne et al. 1997; Wuelker, Plitz, and

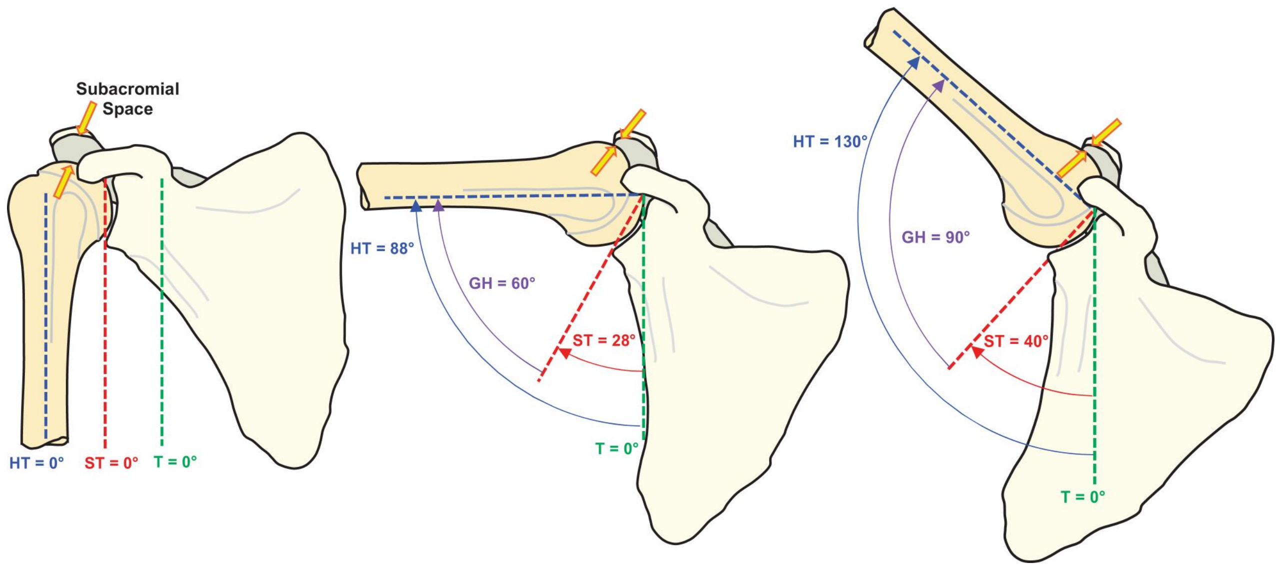

Figure 3. Illustration of scapular rhythm and the associated changes in subacromial space. Impingement begins at 60° GH rotation and full impingement occurs at 90° GH rotation. (Left) The shoulder in the neutral posture with humerothoracic (HT), scapulothoracic (ST) and thoracic (T) angles at 0°. (Middle) HT = 88° is accomplished through ST = 28° and a glenohumeral (GH) of 60°. (Right) HT = 130°, ST = 40° and GH = 90°. The subacromial space is shown between the yellow arrows.

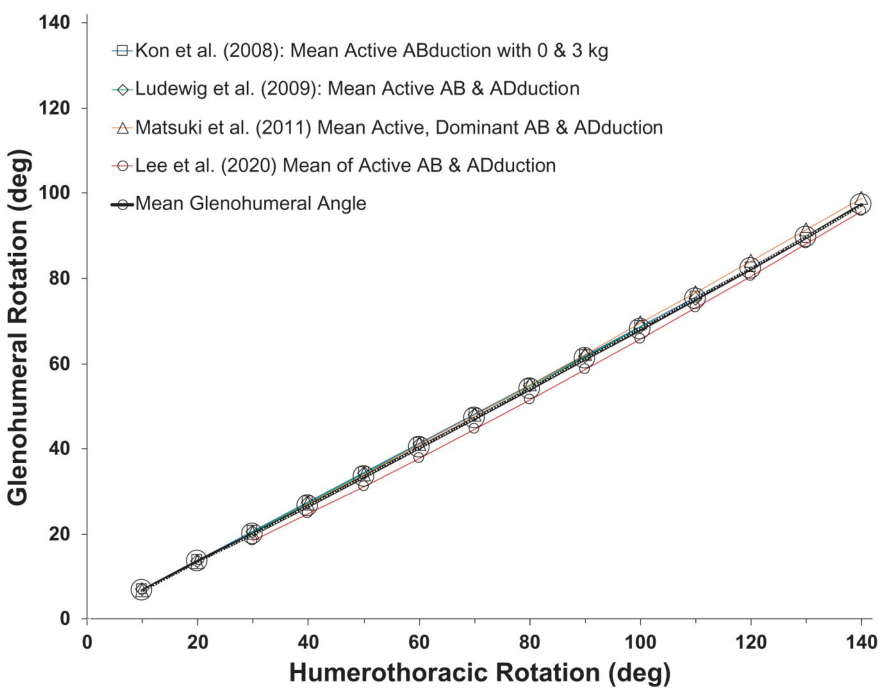

Figure 4. Glenohumeral rotation (GH) angle relative to upper arm rotation (HT) during active abduction and adduction in the four studies referenced and the mean values across the four studies. The second order polynomial equation is shown as a dotted curve and is coincident with the mean curve.

Roetman 1994; Yamamoto et al. 2010). Of these, Yamamoto et al. (2010) provided data with the highest resolution and across the widest range of glenohumeral joint angles; therefore, their *in vitro* data was used to scale manual arm strengths based on glenohumeral rotation in order to control subacromial impingement. They instrumented the coracoacromial arch with thin pressure sensors while the glenohumeral joint was passively rotated in flexion, abduction, rotation, and extension in 10° increments. The contact pressure on the coracoacromial ligament and acromion remained low from 0° to 60° of glenohumeral flexion (GH) then increased approximately linearly from 60° to 90°, and then plateaued to 100°. Thus, no adjustment of manual arm strength is applied for glenohumeral rotations of less than 60° (e.g. approximately 88° of humerothoracic rotation). From 60° to 90° of glenohumeral rotation, the maximum manual arm force was reduced linearly, using a scale factor of 1 for the GH angle of 60° and a factor of 0 for the GH angle of 90° and above. The following Equations (3–5) were used to calculate the scale factor for subacromial impingement (SF_{SI}) based on glenohumeral (GH) angle.

$$\text{For } 0^\circ \leq GH \leq 60^\circ : SF_{SI} = 1 \quad (3)$$

$$\text{For } 60^\circ < GH \leq 90^\circ : SF_{SI} = 1 - \left[\frac{GH-60}{90-60}\right] = 1 - \left[\frac{GH-60}{30}\right] \quad (4)$$

$$\text{For } GH > 90^\circ : SF_{SI} = 0 \quad (5)$$

This model is designed to limit impingement by scaling down the acceptable arm force over the shoulder posture range associated with increasing impingement. This is necessary because as the arm forces increase across this posture range, tendon compression and shear increases. So, the arm forces are reduced to reduce the risk of impingement. The tool allows no hand forces for a GH angle of 90° and above (e.g. approximately 130° of humerothoracic rotation).

2.1.5. Manual arm strength predictions

La Delfa and Potvin (2017) presented the Arm Force Field (AFF) model for estimating right or left manual arm strength based on studies of of 95 healthy, female participants ranging in age from 20 to 62 years (mean: 35.5 ± 12.3 years), stature of 1.660 ± 0.063 m, and weight of 67.1 ± 6.3 kg. The coordinate system was defined with respect to the right shoulder, which was assumed to be located 0.02 m inferior to the acromion when the trunk is upright (Doorenbosch et al. 2001). Hand location was defined by the location of the right knuckle, with the '*x*' axis being the lateral/medial (LM) direction (lateral is positive), the '*y*' axis being the anterior/posterior (AP) direction (anterior is positive), and the '*z*' axis being the superior/inferior (SI) direction (superior is positive). The Arm Force Field method was used to first estimate the 50th percentile female manual arm strength ($MAS_{50th\%}$) in zero gravity in the six primary directions (anterior, posterior, superior, inferior, medial and lateral). Those 50th percentile strengths were then used to estimate the 25th percentile female strength ($MAS_{25th\%}$) assuming a coefficient of variation of 0.276 (La Delfa and Potvin 2017). For each of the hand locations simulated with reaches between 0.20 and 0.55 m ($n = 77$), we used a 50th % female body mass of 73.5 kg and stature of 1.619 m from NHANES 2015–2018; segment lengths, centre of gravities and mass proportions from 3DSSPP v7.1.0; and the assumption that the plane of the arm was vertical to estimate contributions of gravity from the arm, to add to, or subtract from, the AFF manual arm strengths. The RMS differences between the Arm Force Field and empirical strengths, pooled across the 36 hand locations within each of the six directions, were 6.1 N (anterior), 9.7 N (posterior), 5.8 N (superior), 8.8 N (inferior), 7.2 N (medial), and 7.6 N (lateral).

2.1.6. Duty cycle scale factor

The Arm Force Field model provides an estimate of maximum manual arm strengths for single efforts. For repetitive tasks, that may lead to muscle fatigue, it is necessary to further reduce the maximum acceptable force based on the duty cycle (DC). DC is the total duration of efforts in a cycle relative to the total cycle duration, as shown in Equation (6),

$$DC = \frac{(\text{frequency of efforts per cycle})\ (\text{duration per effort})}{(\text{cycle duration})}. \quad (6)$$

The scale factor used to adjust for duty cycle was based on the Maximum Acceptable Effort Equation (MA_{SF}) (Potvin 2012),

$$MAE = 1 - \left[DC - \frac{1}{28,800}\right]^{0.24} \quad (7)$$

2.1.7. Maximum acceptable force

The maximum acceptable force estimated by the tool is calculated using Equation (8),

$$MAF = MAS_{25th\%} * SF_{SI} * SF_{MAE} \quad (8)$$

Where MAF is the maximum acceptable force (N); $MAS_{25th\%}$ is the 25th percentile manual arm strength (N) from Section 2.1.5; SF_{SI} is the subacromial impingement scaling factor from Section 2.1.4; and SF_{MAE} is the fatigue scaling factor from Section 2.1.6.

2.2. Model application and sensitivity

A sensitivity analysis was performed to determine the effects of the model assumptions for (a) scapulohumeral rhythm, (b) range of glenohumeral rotations causing subacromial impingement and (c) upper extremity segment lengths on maximum arm forces. The analyses were performed for all 77 hand locations and for each of the six force directions ($n = 462$).

For scapulohumeral rhythm, the sensitivity analyses compared results using the prior 2nd order polynomial equation for GH angle (see Section 2.1.3 and Figure 4)

Table 1. Summary of the estimated humerothoracic and glenohumeral rotations (deg) for combinations of lateral/medial (ML), anterior (AP) and superior (SI) hand locations in m relative to the shoulder.

Humerothoracic Rotation (deg)

		ML = −0.2 m (Medial)					ML = 0 m					ML = +0.2 m (Lateral)					ML = +0.4 m		
	AP >	0.1	0.2	0.3	0.4	0.5	0.1	0.2	0.3	0.4	0.5	0.1	0.2	0.3	0.4	0.5	0.1	0.2	0.3
SI	**0.5**	131.6					136.4	131.7				131.6							
	0.4	109.8	108.9	111.5			118.3	110.8	109.0			109.8	108.9	111.5					
	0.3	90.6	89.1	90.5	97.4		101.7	91.9	89.0	92.8		90.6	89.1	90.5	97.4		93.7	97.4	
	0.2	70.0	69.1	71.4	78.2		82.7	71.2	69.3	73.9	85.3	70.0	69.1	71.4	78.2		74.9	78.2	85.3
	0.1	45.9	47.7	52.8	61.6	76.2		45.8	48.6	56.4	69.0	45.9	47.7	52.8	61.6	76.2	57.7	61.6	69.0
	0.0	19.3	26.2	35.6	47.4	63.5		16.5	28.2	40.7	55.9	19.3	26.2	35.6	47.4	63.5	42.4	47.4	55.9

Glenohumeral Rotation (deg)

		ML = −0.2 m (Medial)					ML = 0 m					ML = +0.2 m (Lateral)					ML = +0.4 m		
	AP >	0.1	0.2	0.3	0.4	0.5	0.1	0.2	0.3	0.4	0.5	0.1	0.2	0.3	0.4	0.5	0.1	0.2	0.3
SI	**0.5**	90.9					94.4	91.0				90.9							
	0.4	75.2	74.5	76.4			81.3	75.9	74.6			75.2	74.5	76.4					
	0.3	61.6	60.5	61.5	66.4		69.4	62.5	60.5	63.1		61.6	60.5	61.5	66.4		63.8	66.4	
	0.2	47.2	46.6	48.1	52.9		56.0	48.0	46.7	49.9	57.9	47.2	46.6	48.1	52.9		50.6	52.9	57.9
	0.1	30.6	31.9	35.4	41.4	51.5		30.6	32.5	37.8	46.5	30.6	31.9	35.4	41.4	51.5	38.7	41.4	46.5
	0.0	12.7	17.3	23.7	31.6	42.7		10.9	18.7	27.1	37.5	12.7	17.3	23.7	31.6	42.7	28.2	31.6	37.5

Data are shown only for the 77 hand locations with reaches from 0.20 to 0.55 m.

to curves with GH angles 5% lower and 5% higher. For subacromial impingement, four sensitivity analyses were run comparing the SF_{SI} range of 60°–90° (see Section 2.1.4 and Equation (4)) with ranges starting at ±5° (55° and 65°) and ending at ±5° (85° and 95°). For the reach distance of the 50th percentile female of 0.599 m (shoulder to the 2nd knuckle) two sensitivity analyses were run, one using a reach that was 5% shorter (total reach = 0.570 m) and one that was 5% longer (total reach = 0.629 m). For each of the eight sensitivity tests, we calculated the mean differences and RMS differences compared to the maximum acceptable force values for the six directions with values from the original assumptions. These differences were expressed as averages, RMS differences (N) and RMS difference relative to the mean MAF for each direction.

3. Results

3.1. Humerothoracic and glenohumeral rotations for hand locations

For the 77 hand locations, at or above the shoulder, that were within the reach range of the 50th % female (0.20–0.55 m), the mean humerothoracic rotation was 73.7 ± 28.6° (minimum = 16.5°, maximum = 136.4°) and the mean glenohumeral rotation was 50.0 ± 19.9° (minimum = 10.9°, maximum = 94.4°) (Table 1). The humerothoracic and glenohumeral rotations tended to be higher with more superior, more anterior or more extreme lateral hand locations. On average, glenohumeral angles were ~68% of the humerothoracic angles, although that ratio varied with the second order polynomial used to fit the relationship and ranged from ~65% at HT = 0° to 73% at HT = 140°.

3.2. Subacromial impingement scale factors for hand locations

Across all 77 hand locations, the mean impingement scale factor (SI_{SF}) was 0.866 ± 0.269 (range = 1.0–0.0) (Table 2). All conditions with knuckle heights from 0 to 0.2 m ($n = 50$) above the shoulder had SI_{SF} of 1.0, and all heights of 0.3 and above had SI_{SF} values below 1.0. The SI_{SF} values decreased from 0.3 m (mean SI_{SF} = 0.892, $n = 14$) to 0.4 m (mean SI_{SF} = 0.466, $n = 9$) to 0.5 m (all SI_{SF} = 0.0, $n = 4$).

3.3. Maximum acceptable manual arm forces for a single effort after application of the impingement scale factor

The values in Table 3 provide a tool for establishing maximum acceptable manual arm forces for above-shoulder work for a single exertion. After application of the impingement scale factor (Table 2) the maximum acceptable force (MAF) had an average magnitude of 68.6 ± 32.5 N across all 77 hand locations and 6 force directions ($n = 462$) and ranged from 0.0 N (all 24 conditions with the knuckle superior coordinate at 0.5 m) to 162 N (posterior force, with the knuckle −0.2 m medial, 0.5 m anterior and 0.0 m superior to the shoulder) (Table 3).

Table 2. Summary of the subacromial impingement scale factors (range: 0–1), based on glenohumeral rotations for the combinations lateral/medial (ML), anterior (AP) and superior (SI) hand locations in m relative to the shoulder.

		Subacromial Impingement Scale Factor																	
		ML = −0.2 m (Medial)					ML = 0 m					ML = +0.2 m (Lateral)					ML = +0.4 m		
	AP >	0.1	0.2	0.3	0.4	0.5	0.1	0.2	0.3	0.4	0.5	0.1	0.2	0.3	0.4	0.5	0.1	0.2	0.3
SI	0.5	0.000					0.000	0.000				0.000							
	0.4	0.493	0.516	0.453			0.289	0.470	0.512			0.493	0.516	0.453					
	0.3	0.947	0.984	0.951	0.788		0.685	0.917	0.984	0.897		0.947	0.984	0.951	0.788		0.874	0.788	
	0.2	1.000	1.000	1.000	1.000		1.000	1.000	1.000	1.000	1.000	1.000	1.000	1.000	1.000		1.000	1.000	1.000
	0.1	1.000	1.000	1.000	1.000	1.000		1.000	1.000	1.000	1.000	1.000	1.000	1.000	1.000	1.000	1.000	1.000	1.000
	0.0	1.000	1.000	1.000	1.000	1.000		1.000	1.000	1.000	1.000	1.000	1.000	1.000	1.000	1.000	1.000	1.000	1.000

Data are only shown for the 77 hand locations with reaches from 0.20 to 0.55 m.

Table 3. Recommended maximum acceptable forces (N) for single efforts in 6 direction of force application at various combinations of lateral/medial (ML), anterior (AP) and superior (SI) hand locations above the shoulder.

		ML = −0.2 m (Medial)					ML = 0 m					ML = +0.2 m (Lateral)					ML = +0.4 m		
	AP >	0.1	0.2	0.3	0.4	0.5	0.1	0.2	0.3	0.4	0.5	0.1	0.2	0.3	0.4	0.5	0.1	0.2	0.3
Anterior																			
SI	0.5	0					0	0				0							
	0.4	30	42	48			18	32	44			24	30	36					
	0.3	59	72	83	89		48	69	79	91		57	62	67	73		40	42	
	0.2	55	67	76	98		71	73	79	94	131	62	66	69	84		48	47	55
	0.1	47	61	76	98	134		83	100	120	139	58	67	77	91	122	49	46	48
	0.0	43	64	85	108	143		82	96	106	119	64	76	93	109	137	54	51	50
Posterior																			
SI	0.5	0					0	0				0							
	0.4	38	32	24			20	28	27			24	25	26					
	0.3	103	87	65	52		53	70	69	66		58	59	58	57		36	38	
	0.2	117	104	89	88		58	74	87	98	127	60	65	69	81		48	51	66
	0.1	121	120	118	123	140		84	114	132	140	57	69	82	98	131	48	52	64
	0.0	131	137	143	152	162		88	112	123	133	63	79	95	114	150	46	53	65
Superior																			
SI	0.5	0					0	0				0							
	0.4	39	36	29			24	41	39			47	48	39					
	0.3	63	59	50	50		48	71	67	56		79	84	70	55		61	53	
	0.2	62	58	47	53		67	69	62	49	57	71	74	63	52		65	55	48
	0.1	64	62	51	51	65		66	62	45	48	63	66	57	42	45	58	46	42
	0.0	73	73	63	61	73		76	72	53	51	68	69	61	45	49	55	45	42
Inferior																			
SI	0.5	0					0	0				0							
	0.4	76	78	68			35	62	68			64	64	57					
	0.3	147	145	129	110		79	122	125	115		120	119	107	97		95	88	
	0.2	141	136	120	115		108	130	123	111	123	124	120	106	105		104	99	103
	0.1	118	121	107	95	102		123	118	98	99	115	115	101	92	109	94	87	86
	0.0	101	110	99	84	89		116	116	93	84	102	107	96	84	98	82	77	74
Medial																			
SI	0.5	0					0	0				0							
	0.4	34	35	36			21	30	36			30	30	29					
	0.3	78	71	66	65		52	66	65	65		64	62	58	56		53	42	
	0.2	86	76	65	69		62	69	65	62	68	63	66	62	65		78	64	57
	0.1	97	83	69	65	74		65	68	59	59	69	71	69	66	70	114	85	66
	0.0	108	99	83	74	77		80	85	69	60	91	88	83	76	75	132	106	79
Lateral																			
SI	0.5	0					0	0				0							
	0.4	22	27	30			17	25	27			33	30	25					
	0.3	46	56	55	52		38	58	56	49		64	65	50	39		63	50	
	0.2	45	60	59	54		46	61	65	51	48	59	66	60	49		81	71	51
	0.1	58	62	64	50	45		54	68	51	46	58	60	64	48	47	101	82	57
	0.0	71	70	69	51	43		59	68	49	43	59	57	65	47	43	103	90	62

Data are from the 77 hand locations with reaches from 0.20 to 0.55 m.

When pooled within each of the six directions of applied force, the overall means were highest for the inferior direction (96.5 ± 31.0 N), followed by posterior (77.1 ± 40.8 N), anterior (68.9 ± 32.7 N), medial (64.1 ± 24.6 N), superior (53.5 ± 17.2 N) and lateral (51.5 ± 19.9 N).

3.4. Example application with MAE scale factor

An example is provided to show all calculations assuming an anterior force applied with 4 efforts per minute with a duration of 0.8 s/effort, with the hand located laterally at LM = 0.2 m, anteriorly at AP = 0.3 m and superiorly at SI = 0.4 m with respect to the shoulder, with an upright trunk.

The reach (R) would be:

$$R = \sqrt{0.2^2 + 0.3^2 + 0.4^2} = 0.5385 \text{ m}$$

The humerothoracic angle (HT, in deg) is calculated with Equation (1):

$$HT = 90 + \arctan\left[\frac{0.4}{\sqrt{0.2^2 + 0.3^2}}\right] - \arccos\left[\frac{0.305^2 - 0.5385^2 - 0.294^2}{-2(0.5385)(0.294)}\right] = 111.5^\circ$$

The glenohumeral rotation (HT) is estimated with Equation (2):

$$GH = 0.655(111.5) + 0.0002717(111.5^2) = 76.4^\circ$$

The subacromial impingement scale factor (SI_{SF}) is estimated with Equation (4) as $60^\circ \le GH < 90^\circ$:

$$SI_{SF} = 1 - \left[\frac{76.4 - 60}{90 - 60}\right] = 0.453$$

The Arm Force Field model estimated the 50th percentile female manual arm strength to be 86.56 N in zero gravity. Assuming a coefficient of variation of 0.276, the standard deviation is assumed to be (0.276)(86.56) = 23.89 N such that the 25th percentile MAS is estimated to be 86.56 – (0.6745)(23.89) = 70.45 N (La Delfa and Potvin 2017). The weight of the arm was estimated to add 8.67 N to the anterior force so the total 25th percentile manual arm strength was estimated to be 70.45 + 8.67 = 79.12 N. For a single exertion, MAF = ($MAS_{25th\%}$) (SI_{SF}) = (79.12) (0.453) = 35.8 N, which, when rounded, is the same as the associated value of 36 N in Table 3.

Further, assuming a frequency = 4/min and average effort duration = 0.8 s, Equation (6) is used to calculate the duty cycle (DC):

$$DC = \frac{(4 \text{ efforts/min})(0.8 \text{ s/effort})}{60 \text{ s}} = 0.04$$

Equation (7) is then used to calculate the maximum acceptable effort scale factor (MAE_{SF}):

$$MAE_{SF} = 1 - \left[0.04 - \frac{1}{28,800}\right]^{0.24} = 0.538$$

Finally, using Equation (8), the maximum acceptable force (MAF) is calculated with the 25th percentile female manual arm strength ($MAS_{25th\%}$), the subacromical impingement scale factor (SI_{SF}) and the maximum acceptable effort scale factor (SF_{MAE}):

$$MAF = (MAS_{25th\%})\,(SI_{SF})\,(MAE_{SF}) = (79.06)\,(0.453)\,(0.538) = 19.3 \text{ N}$$

Assuming z-scores of −0.6745 for 25th percentile (75% capable) and −1.2816 for 10th percentile (90% capable), the 90% capable values can be estimated by multiplying the values in Table 3 by an additional scale factor of 0.794 before any duty cycle correction. For an all-male workforce, the force limits in the tables would be multiplied by 1.66 (La Delfa and Potvin 2017) to approximate forces that would accommodate 75% of males.

3.4. Sensitivity analyses

The sensitivity analyses demonstrated that all mean, RMS differences and RMS percent differences were of magnitudes less than 4.3 N, 4.1 N and 7.9%, respectively, across the six directions (Table 4). The inferior direction was the most sensitive to the changes based on the mean and RMS difference, and the RMS percent differences were highest with the superior direction. The largest RMS difference, when pooled across directions, was observed when the glenohumeral rotations was decreased by 5%.

4. Discussion

4.1. Major Contributions

An ergonomics assessment tool is presented that provides tables with maximum acceptable force limits for above-shoulder work based on the hand location relative to the shoulder and force direction (anterior, posterior, superior, inferior, medial, and lateral). The limits are based on the strength capabilities of the 25th percentile female and, therefore, should accommodate 75% of female workers and more than 95% of male workers. The tool includes a scale factor for subacromial impingement related to shoulder rotation and a scale factor to control muscle fatigue based on duty cycle. The use of duty cycle, or percent time in an elevated arm position, as a scale factor, is supported by several epidemiologic studies, including studies of shoulder disorders among automobile assembly workers (Punnett et al. 2000) and other workers (Dalbøge et al. 2018).

This new tool fills a need in ergonomics for methods to assess above-shoulder work that are not simply based on gross categories of applied force or shoulder posture. Look-up tables are provided that are easy for practitioners and engineers to use. The tool provides greater precision than existing tools for risk estimation for above-shoulder work and lends itself to

Table 4. Summary of the sensitivity analyses results comparing for developed tool results (Table 3) to results with 2 different scapulohumeral (SH) rhythms, 4 different impingement ranges and 2 different total reaches.

Sensitivity variable	SH rhythm		Impingement range				Total reach	
Range	GH −5%	GH +5%	65–90°	55–90°	60–85°	60–95°	−5%	+5%
Mean Difference (N)								
Anterior	2.3	−2.5	2.0	−2.5	−1.2	1.2	−2.5	2.0
Posterior	1.8	−2.2	1.6	−2.3	−1.0	0.9	−2.1	1.5
Superior	2.5	−2.5	1.9	−2.4	−1.3	1.4	−2.3	2.1
Inferior	**4.1**	**−4.3**	**3.4**	**−4.3**	**−2.2**	**2.2**	**−4.1**	**3.5**
Medial	2.1	−2.3	1.8	−2.3	−1.1	1.1	−2.2	1.8
Lateral	1.8	−1.9	1.5	−1.9	−0.9	0.9	−1.9	1.5
RMS Difference (N)								
Anterior	4.4	4.6	4.2	4.7	2.9	2.6	5.0	4.0
Posterior	3.4	4.0	3.4	4.4	2.4	1.8	3.9	2.9
Superior	4.7	4.5	3.9	4.3	3.1	3.2	4.3	4.0
Inferior	**7.7**	**7.9**	**6.9**	**7.9**	**5.2**	**4.9**	**7.8**	**6.6**
Medial	3.9	4.1	3.7	4.2	2.7	2.3	4.1	3.4
Lateral	3.3	3.5	3.1	3.6	2.2	2.0	3.5	2.9
RMS Difference (% of Mean)								
Anterior	3.1%	3.2%	3.0%	3.3%	2.0%	1.8%	3.5%	2.8%
Posterior	2.1%	2.4%	2.1%	2.7%	1.5%	1.1%	2.4%	1.8%
Superior	**5.5%**	**6.0%**	**4.6%**	**5.7%**	**3.8%**	**3.9%**	**5.6%**	**4.7%**
Inferior	4.9%	5.6%	4.4%	5.6%	3.5%	3.3%	5.5%	4.3%
Medial	2.9%	3.1%	2.8%	3.2%	2.0%	1.7%	3.1%	2.5%
Lateral	3.2%	3.4%	3.1%	3.5%	2.2%	1.9%	3.4%	2.8%

Bolded values are the highest difference magnitudes across the six directions for each variable.

engineering applications for work design. The equations described to estimate glenohumeral rotation and the subacromial impingement scale factor; the manual arm strength based on hand location and force direction; and the maximum acceptable effort scale factor based on duty cycle, can separately, or together, be incorporated directly into digital human modelling software packages to estimate maximum acceptable arm force for any specific hand location within a reach envelope, any force direction, and any population anthropometry. The model equations are provided in this paper, and La Delfa and Potvin (2017) will provide an Arm Force Field Excel spreadsheet and/or MatLab code on request.

4.2. Maximum acceptable force tables for single efforts

For each direction of applied force, the maximum acceptable arm forces (MAFs) tend to decrease as the hand moves superior to the shoulder due predominantly to the subacromial impingement scale factor. However, the strength applied in the inferior direction tended to increase as the hand moved more superior, likely due to the contribution of the latissimus dorsi, until a height of 0.4 above shoulder, when it was countered by the subacromial impingement scale factor (Table 3). On average, the inferior MAFs are ~80% higher than those in the superior direction, likely due again to the additional role of the latissimus dorsi muscles when pulling down with the hand above the shoulder. For both the superior and inferior directions of force application, MAFs are relatively consistent across medial/lateral and anterior hand locations.

For the anterior and posterior directions of applied force, the MAFs increase as the hand moves more anterior to the shoulder, due, in part, to the fact that the elbow joint was always assumed to be below the hand and its moment arm to the force vector decreases as reach distance increases, decreasing the elbow strength demands with greater reach. Anterior and posterior strengths also tend to decrease as the hand moves more medial or lateral to the shoulder because this increases the moment arms of the force vector to the shoulder.

For the medial direction of force application, MAFs were ~25% higher than those in the lateral direction. Medial MAFs remain relatively constant as the hand moves more anterior, but the lateral MAFs were highest between 0 and 0.2 m anterior. Finally, both the medial and lateral MAFs increase as the hand moves more medial or lateral to the shoulder.

Glenohumeral rotation, and thus the impingement scale factor, increases with increasing medial, lateral or superior hand locations (Tables 1 and 2). From shoulder height to 0.2 m above the shoulder there are no adjustments for impingement (scale factor of 1.0). At 0.3 m above the shoulder, 7 of 14 hand locations have minor adjustments (scale factors of 0.77– 0.99). At 0.4 m above the shoulder and higher, all hand locations have an adjustment (scale factors of 0.0–0.52). The adjustments are greatest (scale factor of 0.0) when the hand is 0.5 m above the shoulder, which corresponds to 140 degrees of humerothoracic rotation or close to 90 degrees of glenohumeral rotation, where a high degree of impingement occurs. The model does not allow for any exertions at this level and above, in order to prevent full impingement.

4.3. Sensitivity analyses

The sensitivity analyses indicate relatively small to moderate effects of the adjustment of scapulohumeral rhythm, the range of angles associated with impingement scale factors and the anthropometry-based reach of the arm (Table 4). This indicates that the model was relatively insensitive to the various assumptions made in its design.

4.4. Other methods

As noted in the Introduction, there are few tools for designing above-shoulder work and none of the tools account for population strength capabilities, supraspinatus impingement, and muscle fatigue. When RULA (McAtamney and Corlett 1993) is applied for above shoulder work (shoulder rotation >45 degrees) then the recommendation is always 'further investigation, change may be needed' or 'change may be needed soon'. There is no differentiation between a hand force of 20 N or 100 N, nor force direction, so RULA does not provide specific design limits for over-shoulder work. The same is true for the OCRA risk assessment method recommended in the ISO 11228-3:2007 and 12295:2014 standards (Occhipinti 1998). The method states that if (1) the upper arm is elevated to >80° for >10% of cycle time or >2 actions/min, or (2) the arm is elevated from 45° to 80° deg for >33% of cycle time or >10 actions/min, then further analysis is recommended, but no specific recommendations are made for hand location, hand force or force direction. A recently published shoulder tool estimates cumulative shoulder tendon damage (Hani et al. 2021) but uses only one value for the strength at the shoulder joint, ~77 Nm based on a 50th percentile male, regardless of hand location. Furthermore, that one strength was derived from the 3DSSPP software which was recently shown to predict manual arm strengths that can have very high errors when compared to empirically measured strengths (Hall et al. 2021). The Hani et al. (2021) tool could be modified to incorporate the same manual arm strength and impingement models as used in our tool.

4.5. Accounting for multi-task jobs

Real-world above-shoulder work tasks may change over the course of a day. There are several ways to consider task variation from the design perspective. One is to identify and redesign the worst-case tasks, which are those with the highest ratio of required arm force relative to the maximum acceptable arm force. Another approach when considering the ratio across multiple sub-tasks, is to apply time-weighted averaging (TWA). This may be most effective when the differences in hand position and hand loads are not large. A third approach is to consider the non-linear, cumulative effects of loading and recovery time by applying an approach similar to what is used in the cumulative strain index (CUSI) (Garg, Moore, and Kapellusch 2017), the Distal Upper Extremity Tool (DUET) (Gallagher et al. 2018), and the Recommended Cumulative Recovery Allowance (RCRA) (Gibson and Potvin 2016).

4.6. Assumptions and limitations

Some assumptions and limitations of the various models incorporated into the above-shoulder tool, should be considered. First, the tool is limited to above-shoulder work performed with the trunk essentially upright and would have to be modified to accommodate non-upright trunk postures. Second, the models used to develop the tool include assumptions that may not be applicable to some workplaces, such as workplaces that would not accommodate the 25th percentile female strength. To accommodate 75% of males, a scale factor of 1.66 can be applied that will provide an approximate estimate of MAF values (La Delfa and Potvin 2017). Clearly there are differences between individual workers in strength, anatomy and other physiologic factors that may influence risk. However, like all workplace biomechanical risk assessment models, this one is based on population data and is meant to protect the majority of workers.

The proposed tool assumes that maximum acceptable forces are limited by shoulder strength demands and impingement forces. The models used for scapulohumeral rhythm and the subscapular impingement forces were relatively robust as indicated by the sensitivity analysis. However, the tool should be evaluated with epidemiologic studies of workplaces where tasks frequently require above-shoulder work.

The model does not extend to the area more than 0.5 m above the shoulder due to the limited range of impingement compression data (the data does not extend beyond 90 degrees of glenohumeral rotation or 130 degrees of humerothoracic rotation). Furthermore, when shoulder posture is measured in high-risk occupations (painting, auto assembly, etc.), little work is performed with postures above 90 degrees of humerothoracic rotation (Punnett et al. 2000; Svendsen, Mathiassen, and Bonde 2005).

4.7. Conclusions

A new tool is proposed for designing above-shoulder work that is based on the strength capabilities of the 25th percentile female worker with scaling factors to prevent supraspinatus tendon impingement and shoulder muscle fatigue. The tool estimates hand force limits based on the position of the hand relative to the shoulder, which is relatively easy to measure; therefore, the tool can readily be used by practitioners and other health and safety personnel. The equations from the various models that are integrated into the tool can also be incorporated into existing digital human model software. A sensitivity analysis confirmed that small changes in some of the model assumptions did not substantially impact recommended maximum hand forces. The tool provides for greater precision of acceptable hand forces for specific locations above the shoulder compared to prior upper extremity risk tools and can be readily used by engineers to design above-shoulder work. The ultimate purpose of this assessment tool is to prevent shoulder fatigue, shoulder pain and supraspinatus tears but the ability of this tool to predict these endpoints should be evaluated in epidemiologic studies.

Based on female 50th percentile stature and 25th percentile strength, at the most favourable above shoulder posture, hand forces (direction) should not exceed 143 N (anterior), 162 N (posterior), 84 N (superior), 147 N (inferior), 132 N (medial) and 103 (lateral), when exerted with one hand. These maximum acceptable forces will be further reduced depending on the hand location relative to the shoulder and the duty cycle of the task. Based on this tool, above-shoulder tasks should not be more than 0.47 m above the shoulder, or ~1.80 m above the ground for a 50th percentile female.

Disclosure statement

No potential conflict of interest was reported by the author(s).

Funding

The author(s) reported there is no funding associated with the work featured in this article.

ORCID

David Rempel http://orcid.org/0000-0002-6472-6500
Jim Potvin http://orcid.org/0000-0003-4389-8546

References

ACGIH. 2016. *Upper Limb Localized Fatigue TLV (No. ISBN: 978-1-607261-12-4), TLVs and BEIs Based on the Documentation of the Threshold Limit Values*. Cincinnati, OH: American College of Governmental Industrial Hygienists.

Chopp, J. N., S. L. Fischer, and C. R. Dickerson. 2010. "The Impact of Work Configuration, Target Angle and Hand Force Direction on Upper Extremity Muscle Activity During Sub-Maximal Overhead Work." *Ergonomics* 53 (1): 83–91. doi:10.1080/00140130903323232.

Dalbøge, A., P. Frost, J. H. Andersen, and S. W. Svendsen. 2018. "Surgery for Subacromial Impingement Syndrome in Relation to Intensities of Occupational Mechanical Exposures Across 10-Year Exposure Time Windows." *Occupational and Environmental Medicine* 75 (3): 176–182. doi:10.1136/oemed-2017-104511.

de Groot, J. H., and R. de Brand. 2001. "A Three-Dimensional Regression Model of the Shoulder Rhythm." *JCLB* 16 (9): 735–743. doi:10.1016/S0268-0033(01)00065-1.

Dickerson, C. R., A. C. McDonald, and J. N. Chopp-Hurley. 2020. "Between Two Rocks and in a Hard Place: Reflecting on the Biomechanical Basis of Shoulder Occupational Musculoskeletal Disorders." *Human Factors: The Journal of the Human Factors and Ergonomics Society:* 001872081989619. doi:10.1177/0018720819896191.

Doorenbosch, C. A., A. J. Mourits, D. H. Veeger, J. Harlaar, and F. C. van der Helm. 2001. "Determination of Functional Rotation Axes During Elevation of the Shoulder Complex." *Journal of Orthopaedic & Sports Physical Therapy* 31 (3): 133–137. doi:10.2519/jospt.2001.31.3.133.

Fryar, C. D, M. D, Carroll, Q. Gu, J. Afful, C. L. Ogden. 2021. "Anthropometric Reference Data for Children and Adults: United States, 2015–2018." *Vital Health Stat* 3 (36): 1–44. PMID:33541517.

Fuller, J. R., K. V. Lomond, J. Fung, and J. N. Côté. 2009. "Posture-Movement Changes Following Repetitive Motion-Induced Shoulder Muscle Fatigue." *Journal of Electromyography and Kinesiology : Official Journal of the International Society of Electrophysiological Kinesiology* 19 (6): 1043–1052. doi:10.1016/j.jelekin.2008.10.009.

Gallagher, S., M. C. Schall, R. F. Sesek, and R. Huangfu. 2018. "An Upper Extremity Risk Assessment Tool Based on Material Fatigue Failure Theory: The Distal Upper Extremity Tool (DUET)." *Human Factors: The Journal of the Human Factors and Ergonomics Society* 60 (8): 1146–1162. doi:10.1177/0018720818789319.

Garg, A., J. S. Moore, and J. M. Kapellusch. 2017. "The Composite Strain Index (COSI) and Cumulative Strain Index (CUSI): Methodologies for Quantifying

Biomechanical Stressors for Complex Tasks and Job Rotation Using the Revised Strain Index." *Ergonomics* 60 (8): 1033–1041. doi:10.1080/00140139.2016.1246675.

Gibson, M., and J. R. Potvin. 2016. "An Equation to Calculate the Recommended Cumulative Rest Allowance across Multiple Subtasks.pdf." In *Association of Canadian Ergonomists Conference, Association of Canadian Ergonomists Conference*, Niagara Falls, ON, 1–2.

Grewal, T. -J., and C. R. Dickerson. 2013. "A Novel Three-Dimensional Shoulder Rhythm Definition That Includes Overhead and Axially Rotated Humeral Postures." *Journal of Biomechanics* 46 (3): 608–611. doi:10.1016/j.jbiomech.2012.09.028.

Gupta, R., and T. Q. Lee. 2005. "Positional-Dependent Changes in Glenohumeral Joint Contact Pressure and Force: Possible Biomechanical Etiology of Posterior Glenoid Wear." *Journal of Shoulder and Elbow Surgery* 14 (1): S105–S110. doi:10.1016/j.jse.2004.10.005.

Hall, A. D., N. J. La Delfa, C. Loma, and J. R. Potvin. 2021. "A Comparison Between Measured Female Linear Arm Strengths and Estimates from the 3D Static Strength Prediction Program (3DSSPP)." *Applied Ergonomics* 94: 103415. doi:10.1016/j.apergo.2021.103415.

Hallman, D. M., C. D. N. Rasmussen, M. B. Jørgensen, and A. Holtermann. 2018. "Time Course of Neck-Shoulder Pain among Workers: A Longitudinal Latent Class Growth Analysis." *Scandinavian Journal of Work, Environment & Health* 44 (1): 47–57. doi:10.5271/sjweh.3690.

Hani, D. B., Huangfu, R., Sesek, R., Schall, M. C., Davis, G. A., and Gallagher, S. 2021. "Development and Validation of a Cumulative Exposure Shoulder Risk Assessment Tool Based on Fatigue Failure Theory." *Ergonomics* 64 (1): 39–54. doi:10.1080/00140139.2020.1811399.

Hughes, P. C., R. A. Green, and N. F. Taylor. 2012. "Measurement of Subacromial Impingement of the Rotator Cuff." *Journal of Science and Medicine in Sport* 15 (1): 2–7. doi:10.1016/j.jsams.2011.07.001.

Hyvönen, P., V. Lantto, and P. Jalovaara. 2003. "Local Pressures in the Subacromial Space." *International Orthopaedics* 27 (6): 373–377. doi:10.1007/s00264-003-0488-z.

ISO. 2007. *ISO 11228-3:2007 Manual Handling — Part 3: Handling of Low Loads at High Frequency*. Geneva: International Organization of Standardization.

ISO. 2014. *ISO 12295:2014 Technical Report: Ergonomics – Application Document for International Standards on Manual Handling (ISO 11228-1, ISO 11228-2 and ISO 11228-3) and Evaluation of Static Working Postures (ISO 11226)*. Geneva: International Organization of Standardization.

Jakobsen, E. L. T., K. Biering, A. Kaergaard, and J. H. Andersen. 2018. "Neck–Shoulder Pain and Work Status Among Former Sewing Machine Operators: A 14-year Follow-Up Study." *Journal of Occupational Rehabilitation* 28 (1): 80–88. doi:10.1007/s10926-017-9702-5.

Kon, Y., N. Nishinaka, K. Gamada, H. Tsutsui, and S. A. Banks. 2008. "The Influence of Handheld Weight on the Scapulohumeral Rhythm." *Journal of Shoulder and Elbow Surgery* 17 (6): 943–946. doi:10.1016/j.jse.2008.05.047.

La Delfa, N. J. L., and J. R. Potvin. 2017. "The 'Arm Force Field' Method to Predict Manual Arm Strength Based on Only Hand Location and Force Direction." *Applied Ergonomics* 59 (Pt A): 410–421. doi:10.1016/j.apergo.2016.09.012.

Lee, B., D. Kim, Y. Jang, and H. Jin. 2020. "Three-Dimensional in Vivo Scapular Kinematics and Scapulohumeral Rhythm: A Comparison Between Active and Passive Motion." *Journal of Shoulder and Elbow Surgery* 29 (1): 185–194. doi:10.1016/j.jse.2019.05.036.

Linaker, C. H., and K. Walker-Bone. 2015. "Shoulder Disorders and Occupation." *Best Practice & Research. Clinical Rheumatology* 29 (3): 405–423. doi:10.1016/j.berh.2015.04.001.

Ludewig, P. M., V. Phadke, J. P. Braman, D. R. Hassett, C. J. Cieminski, and R. F. LaPrade. 2009. "Motion of the Shoulder Complex During Multiplanar Humeral Elevation." *The Journal of Bone and Joint Surgery. American Volume* 91 (2): 378–389. doi:10.2106/jbjs.g.01483.

Luo Z. P., H. C. Hsu, J. J. Grabowski, B. F. Morrey, K. N. An. 1998. "Mechanical Environment Associated with Rotator Cuff Tears." *J Shoulder Elbow Surg* 7 (6): 616–620. doi:10.1016/s1058-2746(98)90010-6.

Matsuki, K., K. O. Matsuki, S. Mu, S. Yamaguchi, N. Ochiai, T. Sasho, H. Sugaya, T. Toyone, Y. Wada, K. Takahashi, and S. A. Banks. 2011. "In Vivo 3-Dimensional Analysis of Scapular Kinematics: Comparison of Dominant and Nondominant Shoulders." *Journal of Shoulder and Elbow Surgery* 20 (4): 659–665. doi:10.1016/j.jse.2010.09.012.

McAtamney, L., and E. N. Corlett. 1993. "RULA: A Survey Method for the Investigation of Work-Related Upper Limb Disorders." *Applied Ergonomics* 24 (2): 91–99. doi:10.1016/0003-6870(93)90080-S.

McClure, P. W., L. A. Michener, B. J. Sennett, and A. R. Karduna. 2001. "Direct 3-Dimensional Measurement of Scapular Kinematics during Dynamic Movements In Vivo." *Journal of Shoulder and Elbow Surgery* 10 (3): 269–277. doi:10.1067/mse.2001.112954.

McQuade, K. J., J. Dawson, and G. L. Smidt. 1998. "Scapulothoracic Muscle Fatigue Associated With Alterations in Scapulohumeral Rhythm Kinematics during Maximum Resistive Shoulder Elevation." *The Journal of Orthopaedic and Sports Physical Therapy* 28 (2): 74–80. doi:10.2519/jospt.1998.28.2.74.

McQuade, K. J., S. H. Wei, and G. L. Smidt. 1995. "Effects of Local Muscle Fatigue on Three-Dimensional Scapulohumeral Rhythm." *Clinical Biomechanics (Bristol, Avon)* 10 (3): 144–148. doi:10.1016/0268-0033(95)93704-W.

Miller, M. R., J. Thunes, V. Musahl, S. Maiti, and R. E. Debski. 2019. "A Validated, Specimen-Specific Finite Element Model of the Supraspinatus Tendon Mechanical Environment." *ASME Journal of Biomechanical Engineering* 141 (11): 111003.

Muraki, T., N. Yamamoto, J. W. Sperling, S. P. Steinmann, R. H. Cofield, and K. -N. An. 2017. "The Effect of Scapular Position on Subacromial Contact Behavior: A Cadaver Study." *Journal of Shoulder and Elbow Surgery* 26 (5): 861–869. doi:10.1016/j.jse.2016.10.009.

Occhipinti, E. 1998. "OCRA: A Concise Index for the Assessment of Exposure to Repetitive Movements of the Upper Limbs." *Ergonomics* 41 (9): 1290–1311. doi:10.1080/001401398186315.

Pandey, V., and W. J. Willems. 2015. "Rotator Cuff Tear: A Detailed Update." *Asia-Pacific Journal of Sports Medicine, Arthroscopy, Rehabilitation and Technology* 2 (1): 1–14. doi:10.1016/j.asmart.2014.11.003.

Payne, L. Z., X. -H. Deng, E. V. Craig, P. A. Torzilli, and R. F. Warren. 1997. "The Combined Dynamic and Static Contributions to Subacromial Impingement. A Biomechanical Analysis." *The American Journal of Sports Medicine* 25 (6): 801–808. doi:10.1177/036354659702500612.

Poppen, N. K., and P. S. Walker. 1976. "Normal and Abnormal Motion of the Shoulder." *The Journal of Bone and Joint Surgery. American Volume* 58 (2): 195–201.

Potvin, J. R. 2012. "Predicting Maximum Acceptable Efforts for Repetitive Tasks: An Equation Based on Duty Cycle." *Human Factors* 54 (2): 175–188. doi:10.1177/0018720811424269.

Punnett, L., L J. Fine, W M. Keyserling, G D. Herrin, and D B. Chaffin. 2000. "Shoulder Disorders and Postural Stress in Automobile Assembly Work." *Scandinavian Journal of Work, Environment & Health* 26 (4): 283–291. https://www.jstor.org/stable/40967063. doi:10.5271/sjweh.544.

Rijn, R. M. van., B.M. Huisstede, B. W. Koes, and A. Burdorf. 2010. "Associations Between Work-Related Factors and Specific Disorders of the Shoulder – a Systematic Review of the Literature." *Scandinavian Journal of Work, Environment & Health* 36 (3): 189–201. doi:10.5271/sjweh.2895.

Sirén, M., E. Viikari-Juntura, J. Arokoski, and S. Solovieva. 2019. "Physical and Psychosocial Work Exposures as Risk Factors for Disability Retirement Due to a Shoulder Lesion." *Occupational and Environmental Medicine* 76 (11): 793–800. doi:10.1136/oemed-2019-105974.

Svendsen, S. W., S. E. Mathiassen, and J. P. Bonde. 2005. "Task Based Exposure Assessment in Ergonomic Epidemiology: A Study of Upper Arm Elevation in the Jobs of Machinists, Car Mechanics, and House Painters." *Occupational and Environmental Medicine* 62 (1): 18–26. doi:10.1136/oem.2004.015966.

van der Molen, H. F. van der., C. Foresti, J. G. Daams, M. H. W. Frings-Dresen, and P. P. F. M. Kuijer. 2017. "Work-Related Risk Factors for Specific Shoulder Disorders: A Systematic Review and Meta-Analysis." *Occupational and Environmental Medicine* 74 (10): 745–755. doi:10.1136/oemed-2017-104339.

Wuelker, N., W. Plitz, and B. Roetman. 1994. "Biomechanical Data concerning the Shoulder Impingement Syndrome." *Clinical Orthopaedics and Related Research* 303: 242–249. doi:10.1097/00003086-199406000-00033.

Yamamoto, N., T. Muraki, J. W. Sperling, S. P. Steinmann, E. Itoi, R. H. Cofield, and K. -N. An. 2010. "Contact Between the Coracoacromial Arch and the Rotator Cuff Tendons in Nonpathologic Situations: A Cadaveric Study." *Journal of Shoulder and Elbow Surgery* 19 (5): 681–687. doi:10.1016/j.jse.2009.12.006.

Zheng, M., Z. Zou, P. J. Bartolo, C. Peach, and L. Ren. 2017. "Finite Element Models of the Human Shoulder Complex: A Review of Their Clinical Implications and Modelling Techniques." *International Journal for Numerical Methods in Biomedical Engineering* 33 (2): e02777. doi:10.1002/cnm.2777.